IEEE Access
Multidisciplinary | Rapid Review | Open Access Journal

Received September 10, 2019, accepted October 3, 2019, date of publication October 9, 2019, date of current version October 23, 2019.

Digital Object Identifier 10.1109/ACCESS.2019.2946376

Robust LMedS-Based WLS and Tukey-Based EKF Algorithms Under LOS/NLOS Mixture Conditions

CHEE-HYUN PARK AND JOON-HYUK CHANG, (Senior Member, IEEE)
Department of Electronic Engineering, Hanyang University, Seoul 133-791, South Korea

Corresponding author: Joon-Hyuk Chang (jchang@hanyang.ac.kr)

This work was supported in part by the Research Fund of Signal Intelligence Research Center through the Defense Acquisition Program Administration and the Agency for Defense Development of Korea.

ABSTRACT In this paper, we present robust localization algorithms that use range measurements. The least median of squares (LMedS)-weighted least squares (WLS), LMedS-spherical simplex unscented transform (SSUT) based WLS and Tukey-based extended Kalman filter (EKF) algorithms are proposed for line-of-sight (LOS)/non-line-of-sight (NLOS) mixture environments. First, the LMedS solution is obtained, and then sensors are predicted to be LOS or LOS/NLOS mixture sensors. The range observation predicted as an outlier is replaced with the estimated distance obtained using the LMedS algorithm. Subsequently, the two-step WLS method is executed using these new distance measurements. In the Tukey-based EKF method, Tukey's risk function and the 3-σ edit rule are employed in the innovation step. Furthermore, the mean square error (MSE) analysis of the proposed algorithms is performed. We demonstrate that the positioning accuracy of the proposed methods is higher than that of conventional methods through extensive simulation.

INDEX TERMS Localization, robust, least median of squares, spherical simplex unscented transform, weighted least squares, extended Kalman filter.

I. INTRODUCTION

Source localization is a technique in which the coordinates of the source are determined by utilizing measurements from each sensor, including the time difference of arrival (TDOA), the time of arrival (TOA), the received signal strength (RSS), or the angle of arrival (AOA). Localization of the point target is of considerable interest in various fields of research such as mobile communications, telecommunication, radar and sonar. Position estimation problems in line-of-sight (LOS) environments have been intensely studied in previous works [1]–[6]. However, there are some open problems in this area and a crucial task in location estimation problems is to estimate the source location in LOS/non-line-of-sight (NLOS) mixed situations [7]–[9]. For example, the LOS path between the source and the sensors may be obstructed in indoor or urban scenarios.

Generally, studies regarding location estimation for the LOS/NLOS mixture problem are categorized into three main areas: 1) mathematical optimizations [10]–[13], 2) robust statistics [14]-[19] and 3) LOS and LOS/NLOS mixture sensor identification [20]–[22]. We focus on robust statistics-based localization in this paper. We investigate the robust localization algorithm where the variance of inliers is available. Furthermore, it is well known that the least median of squares (LMedS) estimator demonstrates satisfactory performance when outliers exist [14]–[16]. We utilize the LMedS estimation to eliminate the adverse effects of outliers in the context of LOS/NLOS mixture localization and to obtain an initial solution. Subsequently, the distance between the emitter and the sensor is calculated using this initial solution and each sensor is determined to be an LOS or LOS/NLOS mixture sensor using the initial solution and the 3-σ edit rule [23], [24]. When the sensor is predicted to be an LOS/NLOS mixture sensor, the corresponding observation is replaced with the distance estimated based on the initial solution. In contrast, when the sensor is determined to be an LOS sensor, the corresponding measurement is not altered. Note that we only predict whether the sensor is an LOS or LOS/NLOS mixture sensor using the initial solution and 3-σ edit rule. That is, we do not know exactly whether the sensor is an LOS or LOS/NLOS mixture sensor. Second, the weighting matrix is obtained algebraically or using the spherical simplex unscented transform (SSUT) [25]–[27]. Finally,

The associate editor coordinating the review of this manuscript and approving it for publication was Qinghua Guo.

the proposed LMedS-weighted least squares (WLS) method employing the newly updated distances and the extended Kalman filter (EKF) using Tukey's cost function and 3-σ edit rule are implemented.

The research for the robust estimator has been performed as follows. The TOA-based robust localization using multidimensional similarity (MDS) analysis under LOS/NLOS mixture condition is investigated and its computational complexity is comparatively low [28]. A novel iterative reweighted variational Bayesian learning method based on an off-grid model is presented for impulsive noise processing and it automatically identifies the number of sources without any prior knowledge [29]. In [30], the balancing parameter related to the NLOS error is introduced. The proposed robust method formulation is converted into a nonconvex optimization problem, which is then relaxed into convex semi-definite programming. In [31], the adverse effects of NLOS biases are mitigated by treating them as nuisance parameters through a robust approach, in which the problem dealt with is transformed into a generalized trust region sub-problem using approximations and is solved utilizing a bisection procedure. A Gaussian mixture model (GMM), interacting multiple model (IMM) and EKF are combined into GIMM-EKF [32]. It models the distribution of range estimates for the LOS/NLOS mixture environments, and then a Kalman filter-based IMM framework is introduced with the state probabilities estimated from the GMM. Furthermore, an EKF is employed to determine the emitter position based on the range estimates.

We propose the algorithms based on the three methods, i.e., LMedS, SSUT and EKF for the following reason. The LMedS estimator has been effective for reducing the adverse effects of outliers. However, the auxiliary constraint has not been utilized therein. Therefore, it is expected that the accuracy of the LMedS technique will be enhanced with the incorporation of the two-step WLS method, in which the auxiliary constraint is used. The details of the auxiliary constraint can be found in [2]. The covariance of the outlier-removed statistic is required to apply the constraint. Naturally, the SSUT is utilized for estimating the mean and variance of the outlier-resistant statistic as SSUT is effective for estimating the mean and variance of the nonlinear function. The location accuracy of the LMedS method combined with the two-step WLS and SSUT is superior to that of the LMedS algorithm as can be seen from simulation results. Furthermore, the EKF has been widely used for positioning or tracking. However, accurate positioning is infeasible in the LOS/NLOS mixture environments; thus, we develop the Tukey-based EKF, in which the LMedS solution is used as the initial state vector and Tukey's risk function is utilized in the innovation computation step. We summarize our main contributions as follows:

- We develop robust closed-form localization methods, i.e., LMedS-WLS and LMedS-SSUT WLS, where the LMedS algorithm is adopted as an initial solution to estimate the outlier-resistant distance. Also, the covariance of the outlier-resistant statistic is derived algebraically in the LMedS-WLS algorithm. Furthermore, the covariance of the outlier-removed statistic is computed using the SSUT. It is well known that the performance of the mean and variance estimation obtained utilizing the SSUT is superior to that obtained using the Taylor-series linearization method [25].
- We propose a robust Tukey-based EKF localization method where the innovation is determined based on Tukey's risk function and the 3-σ edit rule. The selection of the initial state vector is important as the estimation performance of the Kalman filter-based methods is much dependent on the initial state vector. The initial state vector is selected as the LMedS solution in the proposed robust EKF.
- The root mean square error (RMSE) performance of the proposed algorithms was superior to those of existing algorithms and close to the Cramér-Rao lower bound (CRLB).
- We analyze the mean square error (MSE) of the proposed methods.

To the best of our knowledge, WLS and SSUT-based approaches combined with the LMedS method have not yet been investigated in the previous works. Furthermore, the EKF-based robust localization method combining Tukey's risk function and the 3-σ edit rule has not been studied. Although there have been studies dealing with the robust EKF, Huber's risk function was utilized therein.

The rest of this paper is organized as follows. Section II discusses the LOS/NLOS mixed location estimation problem to be tackled in this work. Section III describes the existing methods in detail. Section IV presents the proposed positioning algorithms using the two-step WLS, SSUT based on the LMedS method and EKF algorithms based on Tukey's risk function and the 3-σ edit rule. Section V analyzes the MSE of the LMedS-WLS algorithm and the computational complexity of all localization methods. Section VI evaluates the RMSE performances based on the simulation results. Finally, Section VII presents our conclusions.

II. PROBLEM FORMULATION

The aim of the source location method using range measurements is to predict the coordinates of a point target accurately so that the error criterion, e.g., the MSE or sum of squared error, is minimized. In the context of LOS/NLOS mixed source positioning, the measurement equation is determined as

$$r_i = d_i + n_i = \sqrt{(x - x_i)^2 + (y - y_i)^2} + n_i, \qquad (1)$$

where n_i is distributed by $(1-\epsilon)N(0, \sigma_1^2) + \epsilon N(\mu_2, \sigma_2^2)$, $i = 1, 2, \ldots, M$ with M denoting the number of sensors [33]–[36]. The measurement error n_i is a random process that follows a two-mode Gaussian mixture distribution in which the LOS noise component is distributed as $N(0, \sigma_1^2)$ and the NLOS noise follows $N(\mu_2, \sigma_2^2)$ ($N(\mu, \sigma^2)$ denotes a

Gaussian probability density function (PDF) with mean μ and variance σ^2). The LOS noise has a probability of $1-\epsilon$ and the LOS/NLOS noise has a probability of ϵ. Similar to previous LOS/NLOS mixture positioning studies, the mean and variance of the outlier distribution cannot be obtained. Meanwhile, the variance of inlier (σ_1^2) is assumed to be known because it can be estimated by observing the energy bins in the absence of the transmitted signal [37]. Here, ϵ ($0 \leq \epsilon \leq 1$) is a measure of contamination, which is usually lower than 0.1 [33]–[36], $[x \quad y]^T$ represents the unknown source coordinates and $[x_i \quad y_i]^T$ represents the known coordinates of the ith receiver. Furthermore, r_i is the range measurement between the point emitter and the ith receiver and d_i is the true distance between the emitter and ith sensor. Squaring (1) and rearranging yield the following equation:

$$x_i x + y_i y - 0.5R + m_i = 0.5({x_i}^2 + {y_i}^2 - r_i^2), \quad i = 1, 2, \ldots, M, \quad (2)$$

where $R = x^2 + y^2$, $m_i = -d_i n_i - \frac{1}{2} n_i^2$. By representing (2) in a matrix form, we obtain the following

$$\mathbf{A}\mathbf{x} + \mathbf{m} = \mathbf{b}, \quad (3)$$

where $\mathbf{m} = [m_1, \cdots, m_M]^T$, $\mathbf{x} = [x \; y \; R \;]^T$,

$$\mathbf{A} = \begin{pmatrix} x_1 & y_1 & -0.5 \\ \vdots & \vdots & \vdots \\ x_M & y_M & -0.5 \end{pmatrix}, \quad \text{and}$$

$$\mathbf{b} = [b_1 \cdots b_M]^T = \frac{1}{2} \begin{pmatrix} x_1^2 + y_1^2 - r_1^2 \\ \vdots \\ x_M^2 + y_M^2 - r_M^2 \end{pmatrix}.$$

Throughout this paper, a vector is represented with a lowercase boldface letter, a matrix is represented with an uppercase boldface letter and the operator $[\cdot]^T$ denotes a vector/matrix transpose.

III. REVIEW OF THE CONVENTIONAL APPROACHES

A. LMedS ESTIMATOR [14]–[16]

Least sum of squares (LS) has been widely used in statistical signal processing; however, it is vulnerable to outliers that occur in real environments. As an alternative, the LMedS algorithm can be utilized. LMedS estimation is robust to outliers owing to its high breakdown value of 50%. This is the fraction of outliers that can be tolerated while still returning a good solution. The LMedS estimation is summarized in Algorithm 1.

B. EKF

The EKF has been utilized in nonlinear systems and noise models for replacing the Kalman filter. The state transition and observation models are not linear functions of the state but may be differentiable functions. The transition and observation models are represented as follows:

$$\mathbf{x}^{(k)} = \mathbf{f}(\mathbf{x}^{(k-1)}, \mathbf{u}^{(k)}) + \mathbf{w}^{(k)}$$

Algorithm 1 LMedS Estimation

1. Select m random sets of points with size p from the data set, where p is the number of parameters to be estimated.
2. Calculate the LS solution for each subset to find a solution for the parameters from the data set.
3. Calculate the median of the squared residuals for the m random sets.
4. Calculate the minimum value among the median of the squared residuals for the m random sets.
5. The LS solution associated with the minimum value is determined as the LMedS solution.

Algorithm 2 EKF Algorithm

1. Initialize $\mathbf{x}^{(0)}$ and $\mathbf{P}^{(0)}$.
2. Predict state estimate $\widehat{\mathbf{x}}^{(k|k-1)} = \mathbf{f}(\widehat{\mathbf{x}}^{(k-1|k-1)}, \mathbf{u}^{(k)})$.
3. Predict covariance estimate $\mathbf{P}^{(k|k-1)} = \mathbf{F}^{(k)}\mathbf{P}^{(k-1|k-1)}(\mathbf{F}^{(k)})^T + \mathbf{Q}^{(k)}$.
4. Calculate Kalman gain $\mathbf{K}^{(k)} = \mathbf{P}^{(k|k-1)}(\mathbf{H}^{(k)})^T(\mathbf{H}^{(k)}\mathbf{P}^{(k|k-1)}(\mathbf{H}^{(k)})^T + \mathbf{R}^{(k)})^{-1}$.
5. Update state estimate $\widehat{\mathbf{x}}^{(k|k)} = \widehat{\mathbf{x}}^{(k|k-1)} + \mathbf{K}^{(k)}(\mathbf{z}^{(k)} - \mathbf{h}(\widehat{\mathbf{x}}^{(k|k-1)}))$.
6. Update covariance estimate $\mathbf{P}^{(k|k)} = (\mathbf{I} - \mathbf{K}^{(k)}\mathbf{H}^{(k)})\mathbf{P}^{(k|k-1)}$.

$\mathbf{F}^{(k)}$ and $\mathbf{H}^{(k)}$ are the state transition and observation matrices defined as the following Jacobians: $\mathbf{F}^{(k)} = \frac{\partial \mathbf{f}}{\partial \mathbf{x}}|_{\widehat{\mathbf{x}}^{(k-1|k-1)}, \mathbf{u}^{(k)}}$, $\mathbf{H}^{(k)} = \frac{\partial \mathbf{h}}{\partial \mathbf{x}}|_{\widehat{\mathbf{x}}^{(k|k-1)}}$.

$$\mathbf{z}^{(k)} = \mathbf{h}(\mathbf{x}^{(k)}) + \mathbf{v}^{(k)} \quad (4)$$

where $\mathbf{w}^{(k)}$ and $\mathbf{v}^{(k)}$ are the process and observation noises which are assumed to be zero-mean multivariate Gaussian noises with covariance $\mathbf{Q}^{(k)}$ and $\mathbf{R}^{(k)}$, respectively. Furthermore, $\mathbf{u}^{(k)}$ is the input vector. The EKF algorithm is summarized in Algorithm 2.

C. SSUT [25]–[27]

The variance of the estimator can be obtained using the Monte-Carlo (MC) method; however, in this case, tens or hundreds of samples are required. In recent years, the unscented transform (UT) has been utilized as an alternative to the MC method. The number of samples required to estimate the mean is reduced drastically when the UT is utilized. Furthermore, the SSUT has been proposed to reduce the number of samples of the conventional UT, e.g., the UT requires $2n+1$ points whereas the SSUT requires $n+2$ points, where n is the dimension of the parameter to be estimated [25]. Thus, the computational complexity of the SSUT is less than that of the UT as the dimension increases. The SSUT method is summarized in Algorithm 3.

IV. PROPOSED ROBUST LOCALIZATION METHODS

In this section, we present the proposed robust localization methods. The rationale behind the superiority of the proposed methods can be summarized as follows:

Algorithm 3 SSUT

1. Choose $0 \leq W_0 \leq 1$.
2. Choose the weight:
$W_l = (1 - W_0)/(n+1)$.
3. Initialize the vector sequence as:
$e_0^1 = [0]$, $e_1^1 = [-\frac{1}{\sqrt{2W_1}}]$, $e_2^1 = [\frac{1}{\sqrt{2W_1}}]$.
4. Expand vector sequence for $k = 2, \cdots, n$ according to

$$\mathbf{e}_l^k = \begin{cases} \begin{bmatrix} \mathbf{e}_0^{k-1} \\ 1 \end{bmatrix}, & \text{for} l = 0; \\ \begin{bmatrix} \mathbf{e}_l^{k-1} \\ -\frac{1}{\sqrt{k(k+1)W_1}} \end{bmatrix}, & \text{for} l = 1, \cdots, k; \\ \begin{bmatrix} \mathbf{0}_{k-1} \\ \frac{k}{\sqrt{k(k+1)W_1}} \end{bmatrix}, & \text{for} l = k+1, \end{cases}$$

where $\mathbf{e}_l^k$ indicates the lth sigma point of the k-dimension state vector.
5. Select the sigma points as $\aleph_l^k = \widehat{\mathbf{u}} + \sqrt{\mathbf{P}_{uu}}\mathbf{e}_l^k$, where $\widehat{\mathbf{u}}$ is the mean of $\mathbf{u}$ and $\mathbf{P}_{uu}$ is the covariance.
6. Propagate the sigma points through the non-linear function $g(\cdot)$: $\theta_l^k = g(\aleph_l^k)$, $l = 0, \cdots, n+1$.
7. Estimate the mean and covariance of the propagated variable as follows:
$\mathrm{E}[\widehat{\theta}] = \mathrm{E}[g(\mathbf{x})] \simeq \widehat{\theta}_U = \sum_{l=0}^{n+1} W_l^m \theta_l^k$
$\mathrm{Var}[\widehat{\theta}] = \mathrm{Var}[g(\mathbf{x})] \simeq S_U = \sum_{l=0}^{n+1} W_l^c (\theta_l^k - \widehat{\theta}_U)(\theta_l^k - \widehat{\theta}_U)^T$
where $W_l^m = \begin{cases} W_0, & l = 0; \\ \frac{1-W_0}{n+1}, & l = 1, \cdots, n+1. \end{cases}$
$W_l^c = \begin{cases} W_0^m + 1 + \beta - \alpha^2, & l = 0; \\ \frac{1-W_0^m}{n+1}, & l = 1, \cdots, n+1. \end{cases}$
In general, $10^{-4} \leq \alpha \leq 1$ and $\beta = 2$ are the most appropriate when the sample points follow a Gaussian distribution.

1) The error variance of the LMedS solution is calculated and then utilized in the second-step to improve the performance of the LMedS estimate.

2) The auxiliary constraint is further used to enhance the accuracy of the LMedS solution.

3) It is well known that the estimation performance for the Kalman filter-based methods heavily depends on the selection of the initial points. We set the initial point as the LMedS solution, which enhances the accuracy of the Tukey-based EKF. Additionally, Tukey's risk function is employed in the innovation step.

We combine the LMedS technique with the two-step WLS method and SSUT for the following reason. The LMedS method has been utilized as the robust estimator and it has demonstrated a superior performance when the outlier exists if the contamination ratio is less than 0.5. However, the LMedS method does not attain the CRLB because it does not employ the auxiliary constraint. Meanwhile, the two-step WLS algorithm is known to be simple and accurate in LOS conditions, but is vulnerable to LOS/NLOS mixture conditions. Hence, we combine the LMedS method with the two-step WLS algorithm to improve the performance of the LMedS method. Note that the error variance for a nonlinear statistic should be calculated to apply the two-step WLS method. The SSUT is effective for estimating the mean and variance of a nonlinear function. Therefore, the SSUT is combined with the LMedS method for estimating the mean and variance of the nonlinear outlier-resistant statistic. Also, the robust version of the EKF has been widely applied. The LMedS method is combined with the Tukey-based EKF to determine the initial state vector appropriately and is adopted in the calculation of the innovation.

A. THE LMedS-WLS ALGORITHM

Here, we explain the proposed LMedS-WLS method in detail. First, the emitter location is estimated using the LMedS method. Subsequently, the estimated distance between the emitter and the sensor is calculated and then the absolute difference between the range observation and this estimated distance is calculated. If this measure is larger than $3\sigma_1$, the corresponding measurement is substituted as an estimated distance based on the 3-σ edit rule. However, if this measure is smaller than $3\sigma_1$, the corresponding observations are identified as inliers and are unaltered. Then, the two-step WLS localization [2], [3] is performed using these newly updated observations. The first-step WLS estimate is obtained as follows:

$$\hat{\mathbf{x}}_{\mathrm{f}} = (\mathbf{A}^T \mathbf{W}^{\mathrm{n}} \mathbf{A})^{-1} \mathbf{A}^T \mathbf{W}^{\mathrm{n}} \hat{\mathbf{b}}^{\mathrm{n}} \tag{5}$$

where $\hat{\mathbf{b}}^{\mathrm{n}} = [\hat{b}_1^n \cdots \hat{b}_M^n]^T$ and $\hat{b}_i^n$ is defined as follows:

$$\widehat{b}_i^n = \begin{cases} \dfrac{-r_i^2 + x_i^2 + y_i^2}{2}, & \text{if } \mathrm{res}_i \leq 3\sigma_1; \\ \dfrac{-\widehat{r}_i^2 + x_i^2 + y_i^2}{2}, & \text{if } \mathrm{res}_i > 3\sigma_1, \end{cases} \tag{6}$$

$\widehat{r}_i = \sqrt{(\widehat{x}_{\mathrm{LMedS}} - x_i)^2 + (\widehat{y}_{\mathrm{LMedS}} - y_i)^2}$, $[\widehat{x}_{\mathrm{LMedS}}, \widehat{y}_{\mathrm{LMedS}}]^T$ are the estimated coordinates using the LMedS method and $\mathrm{res}_i = |r_i - \widehat{r}_i|$. Also, $\mathbf{W}^{\mathrm{n}} = \mathbf{C}_{\hat{\mathbf{b}}^{\mathrm{n}}}^{-1} = (\mathrm{diag}[\mathrm{Var}\{\hat{b}_1^n\} \cdots \mathrm{Var}\{\hat{b}_M^n\}])^{-1}$ and $\mathrm{Var}\{\hat{b}_i^n\}$ is represented as given below:

$$\mathrm{Var}\{\hat{b}_i^n\} = \begin{cases} r_i^2 \sigma_1^2, & \text{if } \mathrm{res}_i \leq 3\sigma_1; \\ \widehat{r}_i^2 \mathbf{q}_i^T \mathbf{R} \mathbf{q}_i, & \text{if } \mathrm{res}_i > 3\sigma_1 \end{cases} \tag{7}$$

where $\mathbf{q}_i = \left[\frac{\widehat{x}_{\mathrm{LMedS}} - x_i}{g_i}, \frac{\widehat{y}_{\mathrm{LMedS}} - y_i}{g_i}\right]^T$,
$g_i = \sqrt{(\widehat{x}_{\mathrm{LMedS}} - x_i)^2 + (\widehat{y}_{\mathrm{LMedS}} - y_i)^2}$, $\mathbf{R} = [\mathbf{Q}]_{1:2,1:2}$ ($[\mathbf{Q}]_{1:2,1:2}$ denotes the 2×2 submatrix of $\mathbf{Q}$, which excludes the third row and column), $\mathbf{Q} = (\mathbf{A}_L^T \mathbf{A}_L)^{-1} \mathbf{A}_L^T \mathbf{\Phi} \mathbf{A}_L (\mathbf{A}_L^T \mathbf{A}_L)^{-1}$, $\mathbf{A}_L$ denotes the design matrix which is used when the LMedS solution is obtained and $\mathbf{\Phi}$ is defined as follows:

$$[\mathbf{\Phi}]_{i,j} = \begin{cases} \widehat{r}_i^2 \sigma_1^2, & \text{if } i = j; \\ 0, & \text{if } i \neq j. \end{cases} \tag{8}$$

Here, $[\mathbf{\Phi}]_{i,j}$ denotes the (i,j)th element of matrix $\mathbf{\Phi}$. Furthermore, the accuracy of the first-step WLS estimate can be improved in the second-step [2], [3]:

$$\hat{\mathbf{x}}_{\mathrm{f,s}} = (\mathbf{H}^T \mathbf{C}_{\widehat{\mathbf{h}}}^{-1} \mathbf{H})^{-1} \mathbf{H}^T \mathbf{C}_{\widehat{\mathbf{h}}}^{-1} \widehat{\mathbf{h}} \tag{9}$$

where

$$\hat{\mathbf{h}} = \left[[\hat{\mathbf{x}}_f]_1^2 \; [\hat{\mathbf{x}}_f]_2^2 \; [\hat{\mathbf{x}}_f]_3\right]^T, \tag{10}$$

$$\mathbf{H} = \begin{pmatrix} 1 & 1 & 0 \\ 0 & 1 & 1 \\ 1 & 1 & 1 \end{pmatrix}, \text{ and} \tag{11}$$

$$\mathbf{C}_{\hat{\mathbf{h}}} = \text{diag}[2x\ 2y\ 1](\mathbf{A}^T\mathbf{C}_{\hat{\mathbf{b}}^n}^{-1}\mathbf{A})^{-1}\text{diag}[2x\ 2y\ 1] \tag{12}$$

$$\simeq \text{diag}[2[\hat{\mathbf{x}}_f]_1\ 2[\hat{\mathbf{x}}_f]_2\ 1](\mathbf{A}^T\mathbf{C}_{\hat{\mathbf{b}}^n}^{-1}\mathbf{A})^{-1} \times \text{diag}[2[\hat{\mathbf{x}}_f]_1\ 2[\hat{\mathbf{x}}_f]_2\ 1], \tag{13}$$

$[\mathbf{a}]_r$ is the rth component of vector $\mathbf{a}$. The final second-step WLS emitter position estimate is expressed as follows:

$$\hat{\mathbf{x}}_e = \left[\text{sgn}([\hat{\mathbf{x}}_f]_1)\sqrt{[\hat{\mathbf{x}}_{f,s}]_1}\ \ \text{sgn}([\hat{\mathbf{x}}_f]_2)\sqrt{[\hat{\mathbf{x}}_{f,s}]_2}\right]^T \tag{14}$$

where sgn(·) denotes the sign function. The LMedS-WLS localization is summarized in Algorithm 4.

Algorithm 4 LMedS-WLS Algorithm

1. Estimate $[\widehat{x}_{\text{LMedS}}, \widehat{y}_{\text{LMedS}}]^T$ using the LMedS algorithm, where $\widehat{x}_{\text{LMedS}}, \widehat{y}_{\text{LMedS}}$ are estimated x and y coordinates of the emitter utilizing the LMedS algorithm.
2. Calculate $\widehat{r}_i = \sqrt{(\widehat{x}_{\text{LMedS}} - x_i)^2 + (\widehat{y}_{\text{LMedS}} - y_i)^2}$ using the LMedS solution for each sensor ($i = 1, \cdots, M$), where x_i and y_i are the x and y coordinates for the ith sensor.
3. Calculate $\text{res}_i = |r_i - \widehat{r}_i|$ for each sensor.
4. Compare res_i with $3\sigma_1$ for each sensor.
5. If res_i is smaller than $3\sigma_1$, the corresponding measurement is identified as an inlier. The observations predicted as inliers are not altered. On the contrary, when the res_i is larger than $3\sigma_1$, the corresponding observation is replaced with $\widehat{r}_i$.
Namely,

$$\widehat{b}_i^n = \begin{cases} \dfrac{-r_i^2 + x_i^2 + y_i^2}{2}, & \text{if } \text{res}_i \le 3\sigma_1; \\ \dfrac{-\widehat{r}_i^2 + x_i^2 + y_i^2}{2}, & \text{if } \text{res}_i > 3\sigma_1 \end{cases} \tag{15}$$

6. Estimate the emitter position using the two-step WLS algorithm and newly updated measurements.

B. THE LMedS-SSUT BASED WLS ALGORITHM

In this subsection, the LMedS-SSUT based WLS localization algorithm is described in detail. First, the emitter location is estimated using the LMedS method in the same manner as the LMedS-WLS method. Then, the estimated distances between the emitter and the sensors are calculated and then the absolute difference between the range observation and this estimated distance is calculated. If this measure is larger than $3\sigma_1$, the corresponding measurement is substituted as an estimated distance based on the 3σ edit rule. That is, the observations identified as inliers remain unaltered and those predicted as outliers are replaced with the estimated distances. These corrected ranges are used as the mean of sigma points. Consequently, these sigma points are propagated through the nonlinear transform $g(\aleph_{l,i}^k) = \frac{-(\aleph_{l,i}^k)^2 + x_i^2 + y_i^2}{2}$ ($\aleph_{l,i}^k$ is sigma point) and the mean and variance are obtained for these propagated sigma points. Then, two-step WLS localization is performed using the mean and variance of the propagated variable. The LMedS-SSUT based WLS localization is summarized in Algorithm 5.

Algorithm 5 LMedS-SSUT Based WLS Algorithm

1. Estimate $[\widehat{x}_{\text{LMedS}}, \widehat{y}_{\text{LMedS}}]^T$ using the LMedS algorithm.
2. Calculate $\widehat{r}_i = \sqrt{(\widehat{x}_{\text{LMedS}} - x_i)^2 + (\widehat{y}_{\text{LMedS}} - y_i)^2}$ using the LMedS solution for each sensor ($i = 1, \cdots, M$).
3. Calculate $\text{res}_i = |r_i - \widehat{r}_i|$ for each sensor.
4. Compare res_i with the $3\sigma_1$ for each sensor.
5. If res_i is smaller than $3\sigma_1$, the corresponding measurement is identified as an inlier. The observations predicted as inliers are not altered. On the contrary, when the res_i is larger than $3\sigma_1$, the corresponding observation is replaced with $\widehat{r}_i$.
6. The newly updated observations are utilized as the mean for the sigma points of each sensor.
7. Choose $0 \le W_0 \le 1$.
8. Choose the weight: $W_l = (1 - W_0)/(n + 1)$.
9. Initialize the vector sequence as:
$e_0^1 = [0]$, $e_1^1 = [-\frac{1}{\sqrt{2W_1}}]$, $e_2^1 = [\frac{1}{\sqrt{2W_1}}]$.
10. Expand the vector sequence for $k = 2, \cdots, n$ according to

$$\mathbf{e}_l^k = \begin{cases} \begin{bmatrix} \mathbf{e}_0^{k-1} \\ 1 \end{bmatrix}, & \text{for} l = 0; \\ \begin{bmatrix} \mathbf{e}_l^{k-1} \\ -\frac{1}{\sqrt{k(k+1)W_1}} \end{bmatrix}, & \text{for} l = 1, \cdots, k; \\ \begin{bmatrix} \mathbf{0}_{k-1} \\ \frac{k}{\sqrt{k(k+1)W_1}} \end{bmatrix}, & \text{for} l = k+1, \end{cases}$$

where $\mathbf{e}_l^k$ indicates the lth sigma point for the range for each sensor.
11. Select the sigma points as $\aleph_l^k = \mu_r + \sqrt{P_{rr}}\mathbf{e}_l^k$, where μ_r is the newly updated range if the $\text{res}_i > 3\sigma_1$ and original range if the $\text{res}_i \le 3\sigma_1$ and P_{rr} is the variance for the corresponding range.
12. Propagate the sigma points through the non-linear function $g(\cdot)$: $\theta_l^k = g(\aleph_l^k) = \frac{-(\aleph_{l,i}^k)^2 + x_i^2 + y_i^2}{2}$ ($\aleph_{l,i}^k$ is the sigma point):, $l = 0, \cdots, n+1$.
13. Estimate the mean and covariance of the propagated variable as follows:
$\text{E}[\widehat{\theta}] = \text{E}[g(\mathbf{x})] \simeq \widehat{\theta}_U^k = \sum_{l=0}^{n+1} W_l^m \theta_l^k$
$\text{Var}[\widehat{\theta}] = \text{Var}[g(\mathbf{x})] \simeq S_U^k = \sum_{l=0}^{n+1} W_l^c (\theta_l^k - \widehat{\theta}_U)(\theta_l^k - \widehat{\theta}_U)^T$
where $W_l^m = \begin{cases} W_0, & l = 0; \\ \frac{1-W_0}{n+1}, & l = 1, \cdots, n+1. \end{cases}$
$W_l^c = \begin{cases} W_0^m + 1 + \beta - \alpha^2, & l = 0; \\ \frac{1-W_0^m}{n+1}, & l = 1, \cdots, n+1. \end{cases}$
14. Estimate the emitter position using the two-step WLS algorithm, propagated mean and variance. In general, $10^{-4} \le \alpha \le 1$ and $\beta = 2$ are optimal when the sample points follow a Gaussian distribution.

C. TUKEY-BASED EKF ALGORITHM

In the proposed Tukey-based EKF method, Tukey's risk function is utilized when determining the innovation in the state correction step [38]. The Tukey's risk function is defined as follows:

$$\rho(e_i) = \begin{cases} \frac{e_i^2}{2} - \frac{e_i^4}{2c^2} + \frac{e_i^6}{6c^4}, & \text{if } \frac{\text{res}_i}{\sigma_1} \le c; \\ \frac{c^2}{6}, & \text{if } \frac{\text{res}_i}{\sigma_1} > c. \end{cases} \tag{16}$$

The innovation is determined as the derivative of Tukey's loss function ($\rho(e_i)$), known as the influence function in robust statistics [38]. Accordingly, the innovation is calculated as $e_i - \frac{2e_i^3}{c^2} + \frac{e_i^5}{c^4}$ when res_i is smaller than $c\sigma_1$ and as zero when res_i is larger than $c\sigma_1$. When the observation is predicted to be an outlier, the corresponding measurement is not used in the state update because the Kalman gain is very small. That is, the measurement is reflected for the state update proportional to the Kalman gain. The threshold c is set to three according to the 3-σ edit rule. The LMedS solution is utilized as the initial state vector, $\mathbf{Q} = \mathbf{I}_{2\times 2}$ and $\mathbf{R} = \mathbf{I}_{M\times M}$. The Tukey-based EKF algorithm is summarized in Algorithm 6.

Algorithm 6 Tukey-Based EKF Algorithm

1. Set the initial position to the $\mathbf{x}^{(0)} = [\widehat{x}_{\text{LMedS}}, \widehat{y}_{\text{LMedS}}]^T$ and $\mathbf{P}^{(0)} = \mathbf{I}$.
2. Predict state estimate $\widehat{\mathbf{x}}^{(k|k-1)} = \mathbf{F}^{(k)}\widehat{\mathbf{x}}^{(k-1|k-1)}$, where $\mathbf{F}^{(k)} = \mathbf{I}_{2\times 2}$, $\widehat{\mathbf{x}} = [\widehat{x}\ \ \widehat{y}]^T$ and $\widehat{x}, \widehat{y}$ are the estimated location coordinates.
3. Predict covariance estimate $\mathbf{P}^{(k|k-1)} = \mathbf{F}^{(k)}\mathbf{P}^{(k-1|k-1)}(\mathbf{F}^{(k)})^T + \mathbf{Q}^{(k)}$.
4. Calculate $\widehat{r}_i = \sqrt{(\widehat{x}^{(k|k-1)} - x_i)^2 + (\widehat{y}^{(k|k-1)} - y_i)^2}$ for each sensor ($i = 1, \cdots, M$), where $[\widehat{x}^{(k|k-1)}\ \widehat{y}^{(k|k-1)}]^T$ are elements of $\widehat{\mathbf{x}}^{(k|k-1)}$.
5. Calculate $\text{res}_i = |r_i - \widehat{r}_i|$ for each sensor.
6. Compare res_i with the $3\sigma_1$ for each sensor.
7. Calculate the Kalman gain $\mathbf{K}^{(k)} = \mathbf{P}^{(k|k-1)}(\mathbf{H}^{(k)})^T(\mathbf{H}^{(k)}\mathbf{P}^{(k|k-1)}(\mathbf{H}^{(k)})^T + \mathbf{R}^{(k)})^{-1}$, where $\mathbf{H}^{(k)}$ is the Jacobian of $\mathbf{h}^{(k)}$ defined as $\mathbf{H}^{(k)} = \frac{\partial \mathbf{h}}{\partial \mathbf{x}}|_{\widehat{\mathbf{x}}^{(k|k-1)}}$, $\mathbf{h}^{(k)} = [\sqrt{(x^{(k|k-1)} - x_1)^2 + (y^{(k|k-1)} - y_1)^2}, \cdots, \sqrt{(x^{(k|k-1)} - x_M)^2 + (y^{(k|k-1)} - y_M)^2}]^T$.
8. Update the state estimate $\widehat{\mathbf{x}}^{(k|k)} = \widehat{\mathbf{x}}^{(k|k-1)} + \mathbf{K}^{(k)}\mathbf{e}^{(k)}$, where $c = 3$, $\mathbf{e}^{(k)} = [(e_1^n)^{(k)}, \cdots, (e_M^n)^{(k)}]^T$, $(e_i^n)^{(k)} = \begin{cases} e_i^{(k)} - \frac{2(e_i^{(k)})^3}{c^2} + \frac{(e_i^{(k)})^5}{c^4}, & \text{if res}_i \le 3\sigma_1; \\ 0, & \text{if res}_i > 3\sigma_1. \end{cases}$ $e_i^{(k)} = [\mathbf{z}^{(k)} - \mathbf{h}(\widehat{\mathbf{x}}^{(k|k-1)})]_i$ and $[\mathbf{a}]_i$ denotes the ith element of $\mathbf{a}$.
9. Update the covariance estimate $\mathbf{P}^{(k|k)} = (\mathbf{I} - \mathbf{K}^{(k)}\mathbf{H}^{(k)})\mathbf{P}^{(k|k-1)}$.

V. PERFORMANCE ANALYSIS

A. MSE PERFORMANCE ANALYSIS

In this section, we analyze the MSEs of the proposed methods. The MSE is the sum of the squared bias and variance. The RMSE can be obtained by taking the square root of the MSE. The estimation error $\Delta\widehat{\mathbf{x}}_e$ is represented as

$$\begin{aligned} \Delta\widehat{\mathbf{x}}_e & && (17)\\ &= \mathbf{D}_2^{-1}\Delta\widehat{\mathbf{x}}_{\text{f,s}} && (18)\\ &= \mathbf{D}_2^{-1}(\mathbf{H}^T\mathbf{C}_{\widehat{\mathbf{h}}}^{-1}\mathbf{H})^{-1}\mathbf{H}^T\mathbf{C}_{\widehat{\mathbf{h}}}^{-1}(\widehat{\mathbf{h}} - \mathbf{H}\mathbf{x}_{\text{f,s}}) && (19)\\ &= \mathbf{D}_2^{-1}(\mathbf{H}^T\mathbf{C}_{\widehat{\mathbf{h}}}^{-1}\mathbf{H})^{-1}\mathbf{H}^T\mathbf{C}_{\widehat{\mathbf{h}}}^{-1}\mathbf{D}_1(\widehat{\mathbf{x}}_{\text{f}} - \mathbf{x}_{\text{f}}) && (20)\\ &= \mathbf{G}(\mathbf{A}^T\mathbf{C}_{\widehat{\mathbf{b}}^{\text{n}}}^{-1}\mathbf{A})^{-1}\mathbf{A}^T\mathbf{C}_{\widehat{\mathbf{b}}^{\text{n}}}^{-1}(\widehat{\mathbf{b}}^{\text{n}} - \mathbf{A}\mathbf{x}_{\text{f}}) && (21) \end{aligned}$$

where $\mathbf{D}_1 = \text{diag}[2x\ \ 2y\ \ 1]$, $\mathbf{D}_2 = 2\text{diag}[x\ \ y]$, $\mathbf{G} = \mathbf{D}_2^{-1}(\mathbf{H}^T\mathbf{C}_{\widehat{\mathbf{h}}}^{-1}\mathbf{H})^{-1}\mathbf{H}^T\mathbf{C}_{\widehat{\mathbf{h}}}^{-1}\mathbf{D}_1$ and $\mathbf{x}_{\text{f}}$, $\mathbf{x}_{\text{f,s}}$ are the true values for $\widehat{\mathbf{x}}_{\text{f}}$, $\widehat{\mathbf{x}}_{\text{f,s}}$. Then, the error covariance matrix of $\widehat{\mathbf{x}}_e$ is represented as follows:

$$\text{cov}[\Delta\widehat{\mathbf{x}}_e^{\text{LMedS-WLS}}] = \mathbf{G}(\mathbf{A}^T\mathbf{C}_{\widehat{\mathbf{b}}^{\text{n}}}^{-1}\mathbf{A})^{-1}\mathbf{G}^T. \tag{22}$$

As $E[\widehat{\mathbf{h}}] \simeq \mathbf{h}$ in a sufficiently small noise condition, the bias for the second step estimate of the LMedS-WLS method is approximately the zero vector. Thus, the bias of the final solution for the LMedS-WLS algorithm is the zero vector. Then, $\text{MSE}(\hat{\mathbf{x}}_{\text{e}}) \simeq \text{tr}[\text{cov}(\hat{\mathbf{x}}_{\text{e}})]$, where $\text{tr}(\cdot)$ denotes the trace operator. The MSE performance for the LMedS-SSUT WLS method can be analyzed in the same manner. The covariance of the LMedS-SSUT WLS algorithm is derived as follows:

$$\text{cov}[\Delta\widehat{\mathbf{x}}_e^{\text{LMedS-SSUT WLS}}] = \mathbf{G}(\mathbf{A}^T\mathbf{C}_{\widehat{\mathbf{b}}^{\text{s}}}^{-1}\mathbf{A})^{-1}\mathbf{G}^T \tag{23}$$

where $\mathbf{C}_{\hat{\mathbf{b}}^s} = \text{diag}[\text{Var}(\hat{\theta}_{U,1}), \cdots, \text{Var}(\hat{\theta}_{U,M})]$, $\hat{\mathbf{b}}^s = [\hat{\theta}_{U,1}, \cdots, \hat{\theta}_{U,M}]^T$, $\hat{\theta}_{U,i}$ is the same as that defined in Algorithm 5.13 and the subscript i indicates the sensor index. $\text{Var}(\hat{\theta}_{U,i})$ can be derived as follows:

$$\text{Var}(\hat{\theta}_{U,i}) = \sum_{l=0}^{n+1}(W_{l,i}^m)^2 S_{U,i}^k \tag{24}$$

where $W_{l,i}^m$ and $S_{U,i}^k$ are the same as those defined in Algorithm 5.13. Furthermore, the state error covariance can be utilized as the MSE performance of the Tukey-based EKF algorithm. Namely, the MSE of the Tukey-based EKF can be approximated as

$$\mathbf{P}^{(k|k)} = (\mathbf{I} - \mathbf{K}^{(k)}\mathbf{H}^{(k)})\mathbf{P}^{(k|k-1)}. \tag{25}$$

B. COMPUTATIONAL COMPLEXITY ANALYSIS

Table 1 shows the computational complexity of the existing and proposed robust algorithms, where M is the number of sensors, p is the number of parameters and I is the iteration number. The computational complexity is dependent on the matrix inverse and multiplication operations because their computational load is higher than that of other operations. The computational complexities of the proposed LMedS-WLS and LMedS-SSUT WLS methods were higher than that of the LMedS algorithm owing to the incorporation of the two-step WLS procedure. Furthermore, the computational burden of the Tukey-based EKF algorithm was higher

TABLE 1. Comparison of the computational complexity.

Algorithm	Computational complexty
LMedS-WLS	$O(M^3 + p^2M + pM^2 + p^3)$
LMedS-SSUT	$O(M^3 + p^2M + pM^2 + 2p^3)$
Tukey-based EKF	$O(I(M^3 + p^3))$
LMedS	$O(M^3)$
Bi-section	$2 \times O(IM)$
MCC-EKF	$O(I(M^3 + p^3))$

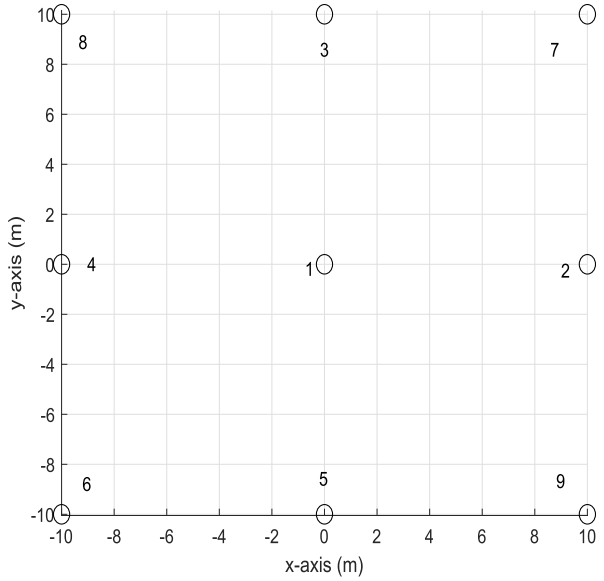

FIGURE 1. Deployment of sensors.

than that of the LMedS method. However, the computational complexities of all methods, excluding the bi-section method, are approximately determined as $O(M^3)$ because p is relatively small compared with M. Therefore, the proposed methods have competitive advantages in both localization accuracy and computational complexity compared to the other algorithms. Although the proposed algorithms require the matrix inverse operation, inverse matrix may be updated intermittently in slowly varying environments. Consequently, the computational complexity can be considerably reduced.

VI. SIMULATION RESULTS

We compared the performance of the proposed LOS/NLOS mixed emitter positioning methods with those of a robust LMedS method [16], a bi-section estimator [39] and a maximum correntropy criterion (MCC)-EKF technique [40] in this section. The simulation settings are shown in Table 2.

The RMSE is defined as follows:

$$\text{RMSE} = \sqrt{\frac{\sum_{i=1}^{10}\sum_{k=1}^{200}[(\hat{x}^k(i) - x(i))^2 + (\hat{y}^k(i) - y(i))^2]}{10 \times 200}} \tag{26}$$

where $[\hat{x}^k(i),\ \hat{y}^k(i)]^T$ is the estimated location of the point target in the ith position set and kth iteration. Additionally, $x(i)$ and $y(i)$ denote the ith true coordinates of the emitter. Fig. 1 shows the arrangement of the receivers. Although we

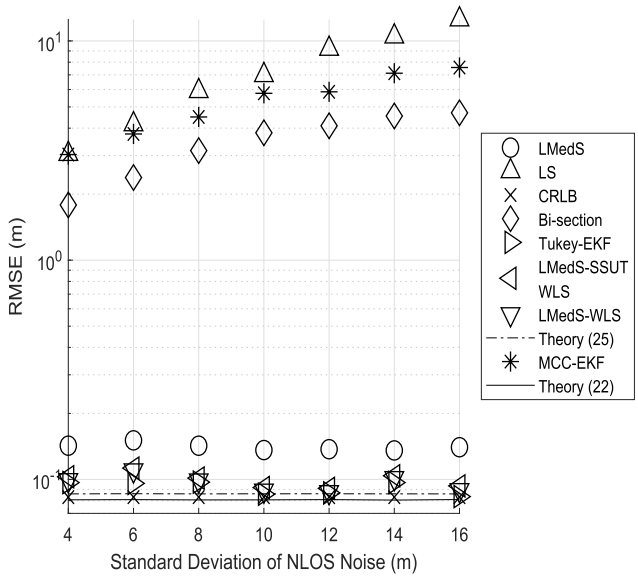

(a) bias of NLOS noise (μ_2): 4 m, standard deviation of LOS noise (σ_1): 0.1 m

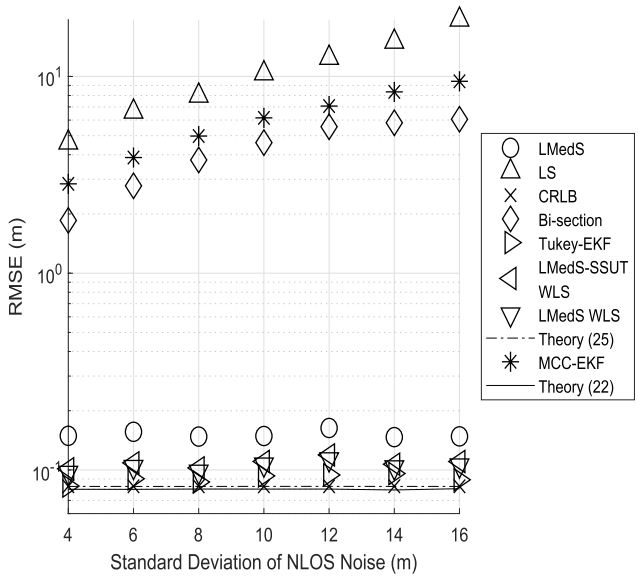

(b) σ_1: 0.1 m, μ_2: 4 m

FIGURE 2. Comparison of the RMSEs of the proposed estimators with those of existing methods (a) RMSE in the case that sensors 8 and 9 are LOS/NLOS mixture sensors and the remaining sensors are LOS sensors (b) RMSE in the case that sensors 7, 8 and 9 are LOS/NLOS mixture sensors and the remaining sensors are LOS sensors.

used a fixed sensor deployment in this simulation, the RMSE performance varies according to the geometry of the sensors. This observation can be justified based on the concept of geometric dilution of precision (GDOP) (the localization accuracy improves as the GDOP decreases).

The localization accuracy with respect to the standard deviation of the NLOS error is displayed in Fig. 2. In Fig. 2(a), sensors 8 and 9 were the LOS/NLOS mixture sensors and the remaining sensors were LOS sensors. The bias of the

TABLE 2. Simulation settings.

Parameter	Explanation
Source location	a single source located within a 20×20 m^2 region
Number of simulated sources	10
Number of Monte-Carlo simulation	200
LOS noise variance of each sensor	assumed to be identical
Number of receivers	9
Directivity of source	omni-direction

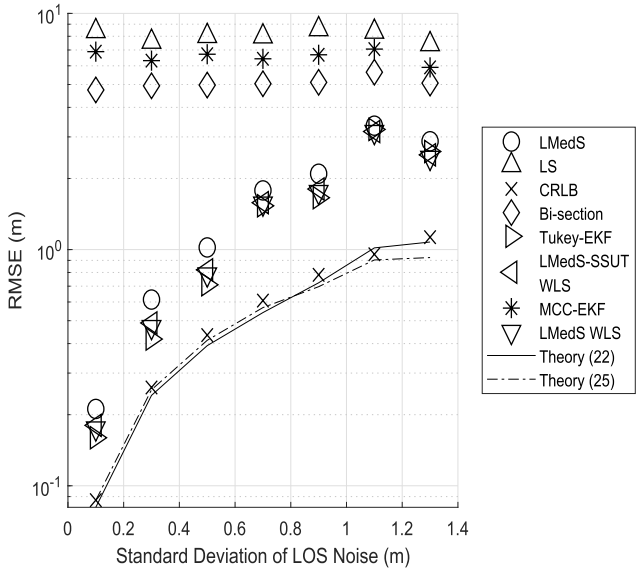

FIGURE 3. RMSEs of the localization algorithms as a function of standard deviation of LOS noise (bias of NLOS noise (μ_2): 4 m, standard deviation of NLOS noise (σ_2): 10 m).

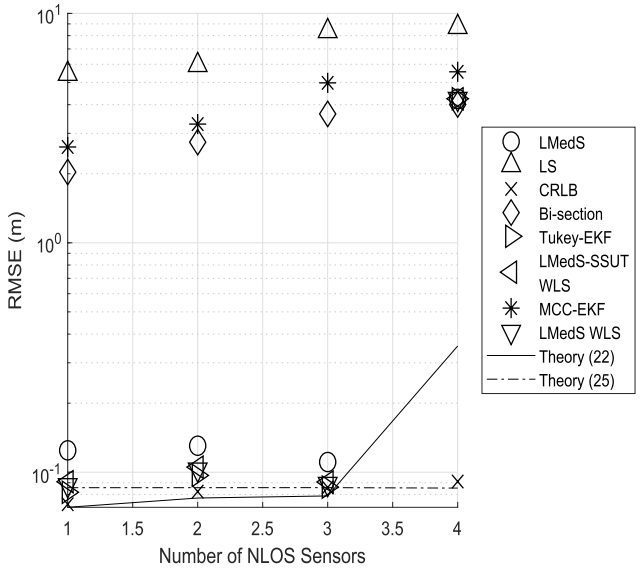

FIGURE 4. RMSEs of the localization algorithms as a function of the number of NLOS sensors (bias of NLOS noise (μ_2): 4 m, standard deviation of LOS noise (σ_1): 0.1 m, standard deviation of NLOS noise (σ_2): 10 m).

NLOS error (μ_2) was 4 m, and the standard deviation of the LOS noise (σ_1) was 0.1 m. Further, the initial states of the EKF were set to the LMedS solution in the Tukey-based EKF method. It is evident that the RMSEs of the proposed robust WLS methods were lower than those of the other existing methods. The RMSEs of the proposed algorithms were approximately 0.09 m and the RMSEs of the LMedS, bi-section and MCC-EKF methods were about 0.15 m, 2.0-4.0 m and 3.0-7.5 m in Fig. 2(a), respectively. The proposed methods outperformed the LMedS, bi-section and MCC-EKF methods by approximately 0.06 m, 1.91-3.91 m and 2.91-6.41 m, respectively. The RMSEs of the proposed methods were nearly the same. The CRLB was obtained using the MC integration techniques explained in [34]. The CRLB was 0.08 m and the RMSEs of the proposed methods were larger than the CRLB by 0.01 m. The theoretical values ((22) and (25)) were approximately the same as the CRLB.

In Fig. 2(b), sensors 7, 8 and 9 were LOS/NLOS mixture sensors, whereas the remaining environments were identical to those in Fig. 2(a). The RMSEs of the proposed methods were approximately 0.12 m and the RMSEs of the LMedS, bi-section and MCC-EKF methods were approximately 0.17 m, 2-6 m and 3-10 m, respectively. In Fig. 2(b), the proposed methods outperformed the LMedS, bi-section and MCC-EKF methods by approximately 0.05 m, 1.88-5.88 m and 2.88-9.88 m, respectively. The CRLB was about 0.1 m and the RMSEs of the proposed methods were larger than the CRLB by 0.07 m. The CRLB was approximately the same as the theoretical value attained from (22) and (25).

Fig. 3 shows the RMSEs versus the standard deviation of inliers. In Fig. 3, sensors 7, 8 and 9 were assumed to be LOS/NLOS mixture sensors and the remaining sensors were assumed to be LOS sensors. The RMSEs of the proposed methods were lower than those of the other methods in Fig. 3. The performance of all the robust methods became worse as the standard deviation of the LOS error increased. The RMSEs of the proposed methods approximated the CRLB in the small LOS noise regimes, but were moderately degraded than the CRLB under high LOS noise conditions.

Next, Fig. 4 illustrates the RMSEs versus the number of LOS/NLOS mixture sensors. The proposed robust WLS-based methods outperformed the other methods, as shown in Fig. 4. When the number of LOS/NLOS mixture sensors was larger than three, the RMSEs of all the robust WLS methods were significantly increased. Note that the theoretical breakdown point of the LMedS algorithm is $\frac{\lfloor((M-(p+1))/2\rfloor+1}{M}$, where $\lfloor a \rfloor$ is an integer part of a [14]. The theoretical breakdown point of the LMedS method in this study is 33.3 % because $M = 9$ and $p = 3$. Thus, it can

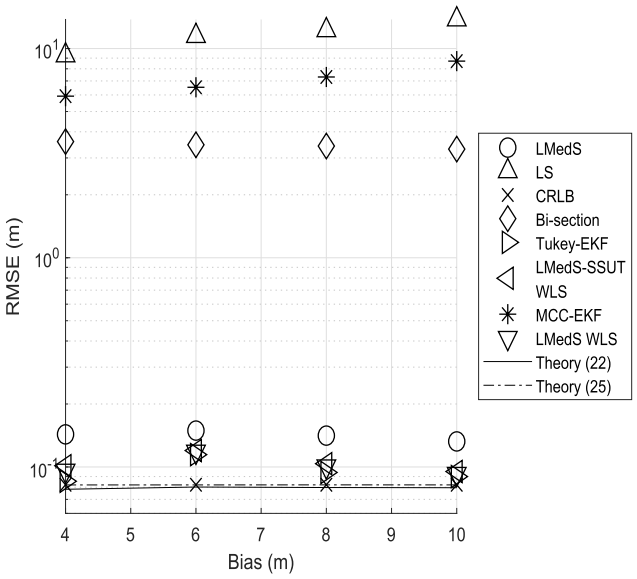

FIGURE 5. RMSEs of the localization algorithms as a function of the bias in the case that sensors 7, 8 and 9 are LOS/NLOS mixture sensors and the remaining sensors are LOS sensors (standard deviation of LOS noise (σ_1): 0.1 m, standard deviation of NLOS noise (σ_2): 10 m).

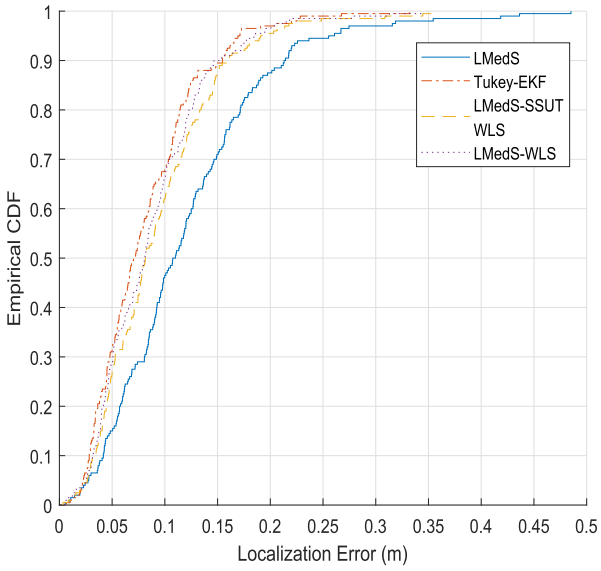

FIGURE 6. Empirical cumulative distribution function (ECDF) of the estimation error for robust localization methods in the case that sensors 7, 8 and 9 are LOS/NLOS mixture sensors and the remaining sensors are LOS sensors (standard deviation of LOS noise (σ_1): 0.1 m, standard deviation of NLOS noise (σ_2): 10 m.

be observed that the simulation results were consistent with the theoretical value. The RMSEs of the proposed methods increased as the number of LOS/NLOS mixture sensors increased, but were lower than those of the existing methods.

Fig. 5 shows the RMSEs versus bias. The RMSEs of all the methods were approximately constant as the bias varied and the proposed methods outperformed the other existing algorithms. Namely, the localization performances of the proposed WLS-based algorithms were not affected by the bias

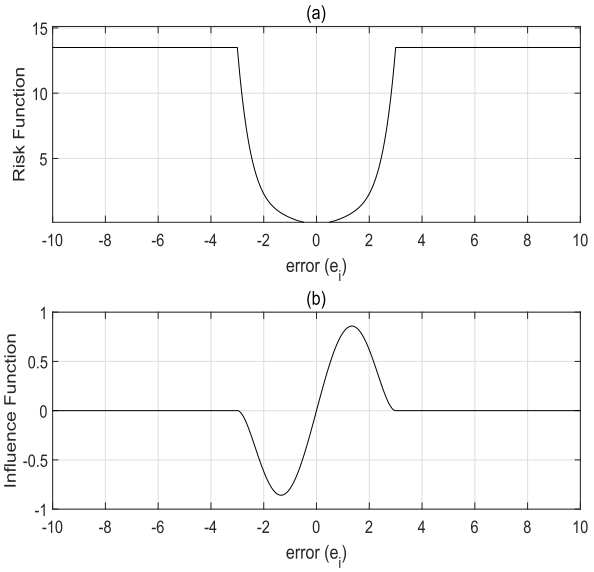

FIGURE 7. Risk and influence function of the Tukey-based EKF algorithm (a) Risk function (b) Influence function.

because the localization estimate was dependent on the LOS sensors.

The empirical cumulative distributive function (ECDF) for the localization methods is displayed in Fig. 6 when sensors 7, 8 and 9 were LOS/NLOS mixture sensors. The proposed methods outperformed the LMedS algorithm and the Tukey-based EKF localization method was superior to the other proposed algorithms.

Fig. 7 shows the risk and influence function for the Tukey-based EKF localization method. When the estimation error is larger than a certain threshold, the loss function is clipped to a constant. Furthermore, the influence function, which is the derivative of the risk function, redescends towards zero when the estimation error surpasses the threshold. Therefore, the proposed Tukey-based EKF algorithm is less sensitive to the outliers compared with the non-robust algorithm, in which the risk function is typically a square function.

VII. CONCLUSION

Novel robust localization methods were developed utilizing the LMedS-WLS, LMedS-SSUT WLS and Tukey-based EKF algorithms. First, the LMedS solution was obtained and the distance measurements were updated. That is, the observation predicted as the outlier was replaced with the distance estimated using the LMedS algorithm. The proposed LMedS-WLS and LMedS-SSUT WLS methods employed the weighting matrix determined based on this LMedS solution. Furthermore, the Tukey-based EKF method utilized the Tukey's risk function and 3-σ edit rule for determining the innovation. The RMSE performances of the proposed LMedS-WLS, LMedS-SSUT WLS and Tukey-based EKF methods were determined to be superior to those of existing algorithms. Furthermore, the theoretical MSE performance of the proposed localization algorithms was analyzed and

the computational complexity was investigated for all the localization methods.

REFERENCES

[1] D. J. Torrieri, "Statistical theory of passive location systems," *IEEE Trans. Aerosp. Electron. Syst.*, vol. AES-20, no. 2, pp. 183–198, Jun. 1983.

[2] Y. T. Chan and K. C. Ho, "A simple and efficient estimator for hyperbolic location," *IEEE Trans. Signal Process.*, vol. 42, no. 8, pp. 1905–1915, Aug. 1994.

[3] H. C. So and L. Lin, "Linear least squares approach for accurate received signal strength based source localization," *IEEE Trans. Signal Process.*, vol. 59, no. 8, pp. 4035–4040, Aug. 2011.

[4] C.-H. Park and J.-H. Chang, "Closed-form localization for distributed MIMO radar systems using time delay measurements," *IEEE Trans. Wireless Commun.*, vol. 15, no. 2, pp. 1480–1490, Feb. 2016.

[5] C. -H. Park, and J.-H. Chang, "Shrinkage estimation-based source localization with minimum mean squared error criterion and minimum bias criterion," *Digit. Signal Process.*, vol. 29, pp. 100–106, Jun. 2014.

[6] J. A. Belloch, A. Gonzalez, A. M. Vidal, and M. Cobos, "On the performance of multi-GPU-based expert systems for acoustic localization involving massive microphone arrays," *Expert Syst. Appl.*, vol. 42, no. 13, pp. 5607–5620, Aug. 2015.

[7] I. Guvenc and C.-C. Chong, "A survey on TOA based wireless localization and NLOS mitigation techniques," *IEEE Commun. Surveys Tuts.*, vol. 11, no. 3, pp. 107–124, Aug. 2009.

[8] A. M. Zoubir, V. Koivunen, Y. Chakhchoukh, and M. Muma, "Robust estimation in signal processing: A tutorial-style treatment of fundamental concepts," *IEEE Signal Process. Mag.*, vol. 29, no. 4, pp. 61–80, Jul. 2012.

[9] N. Kbayer and M. Sahmoudi, "Performances analysis of GNSS NLOS bias correction in urban environment using a three-dimensional city model and GNSS simulator," *IEEE Trans. Aerosp. Electron. Syst.*, vol. 54, no. 4, pp. 1799–1814, Aug. 2018.

[10] S. Zhang, S. Gao, and G. Wang, "Robust NLOS error mitigation method for TOA-based localization via second-order cone relaxation," *IEEE Commun. Lett.*, vol. 19, no. 12, pp. 2210–2213, Dec. 2015.

[11] G. Wang, H. Chen, Y. Li, and N. Ansari, "NLOS error mitigation for TOA-based localization via convex relaxation," *IEEE Trans. Wireless Commun.*, vol. 13, no. 8, pp. 4119–4131, Aug. 2014.

[12] R. M. Vaghefi, J. Schloemann, and R. M. Buehrer, "NLOS mitigation in TOA-based localization using semidefinite programming," in *Proc. IEEE WPNC*, Mar. 2013, pp. 1–6.

[13] R. M. Vaghefi and R. M. Buehrer, "Cooperative localization in NLOS environments using semidefinite programming," *IEEE Commun. Lett.*, vol. 19, no. 8, pp. 1382–1385, Aug. 2015.

[14] P. J. Rousseeuw and A. M. Leroy, *Robust Regression and Outlier Detection*. Hoboken, NJ, USA: Wiley, 1987.

[15] Z. Li, W. Trappe, Y. Zhang, and B. Nath, "Robust statistical methods for securing wireless localization in sensor networks," in *Proc. IEEE Int. Symp. Inf. Process. Sensor Netw.* Los Angeles, CA, USA, Apr. 2005, pp. 91–98.

[16] R. Casas, A. Marco, J. J. Guerrero, and J. Falco, "Robust estimator for non-line-of-sight error mitigation in indoor localization," *EURASIP J. Adv. Signal Process.*, vol. 2006, Dec. 2006, Art. no. 43429.

[17] C. H. Park, S. Lee, and J.-H. Chang, "Robust closed-form time-of-arrival source localization based on α-trimmed mean and Hodges–Lehmann estimator under NLOS environments," *Signal Process.*, vol. 111, pp. 113–123, Jun. 2015.

[18] X.-W. Chang and Y. Guo, "Huber's M-estimation in relative GPS positioning: Computational aspects," *J. Geodesy*, vol. 79, nos. 6–7, pp. 351–362, Aug. 2005.

[19] J. L. Hodges and E. L. Lehmann, "Estimates of location based on rank tests," *Ann. Math. Stat.*, vol. 34, no. 2, pp. 598–611, 1963.

[20] I. Guvenc, C. Chong, F. Watanabe, and B. Nath, "NLOS identification and mitigation for UWB localization systems," in *Proc. IEEE Wireless Commun. Netw. Conf.*, Kowloon, China, Mar. 2007, pp. 1571–1576.

[21] Y.-T. Chan, W.-Y. Tsui, H.-C. So, and P.-C. Ching, "Time-of-arrival based localization under NLOS conditions," *IEEE Trans. Veh. Technol.*, vol. 55, no. 1, pp. 17–24, Jan. 2006.

[22] S. Gezici, H. Kobayashi, and H. V. Poor, "Nonparametric nonline-of-sight identification," in *Proc. IEEE Veh. Technol. Conf.*, Orlando, FL, USA, Mar. 2003, pp. 2544–2548.

[23] C. Leys, C. Ley, O. Klein, P. Bernard, and L. Licata, "Detecting outliers: Do not use standard deviation around the mean, use absolute deviation around the median," *J. Exp. Social Psychol.*, vol. 49, no. 4, pp. 764–766, 2013.

[24] J. Miller, "Reaction time analysis with outlier exclusion: Bias varies with sample size," *Quart. J. Exp. Psychol.*, vol. 43, no. 4, pp. 907–912, 1991. doi: 10.1080/14640749108400962.

[25] S. J. Julier and J. K. Uhlmann, "Unscented filtering and nonlinear estimation," *Proc. IEEE*, vol. 92, no. 3, pp. 401–422, Mar. 2004.

[26] S. J. Julier, "The spherical simplex unscented transformation," in *Proc. Amer. Control Conf.*, Denver, CO, USA, Jun. 2003, pp. 2430–2434.

[27] Z. Fangfang, S. G. Shuzhi, Z. Jie, and H. Wei, "Celestial navigation in deep space exploration using spherical simplex unscented particle filter," *IET Signal Process.*, vol. 12, no. 4, pp. 463–470, Jun. 2018.

[28] W. Xiong and H. C. So, "TOA-based localization with NLOS mitigation via robust multidimensional similarity analysis," *IEEE Signal Process. Lett.*, vol. 26, no. 9, pp. 1334–1338, Sep. 2019.

[29] F. Ma, C. Xu, X. Zhang, J. He, and W. Su, "Iterative reweighted DOA estimation for impulsive noise processing based on off-grid variational Bayesian learning," *IEEE Access*, vol. 7, pp. 104642–104654, 2019.

[30] H. Chen, G. Wang, and N. Ansari, "Improved robust TOA-based localization via NLOS balancing parameter estimation," *IEEE Trans. Veh. Technol.*, vol. 68, no. 6, pp. 6177–6181, Jun. 2019.

[31] S. Tomic and M. Beko, "A robust NLOS bias mitigation technique for RSS-TOA-based target localization," *IEEE Signal Process. Lett.*, vol. 26, no. 1, pp. 64–68, Jan. 2019.

[32] W. Cui, B. Li, L. Zhang, and W. Meng, "Robust mobile location estimation in NLOS environment using GMM, IMM, and EKF," *IEEE Syst. J.*, vol. 13, no. 3, pp. 3490–3500, Sep. 2019.

[33] F. Yin, C. Fritsche, F. Gustafsson, and A. M. Zoubir, "EM- and JMAP-ML based joint estimation algorithms for robust wireless geolocation in mixed LOS/NLOS environments," *IEEE Trans. Signal Process.*, vol. 62, no. 1, pp. 168–182, Jan. 2014.

[34] Y. Feng, C. Fritsche, F. Gustafsson, and A. M. Zoubir, "TOA-based robust wireless geolocation and Cramér-Rao lower bound analysis in harsh LOS/NLOS environments," *IEEE Trans. Signal Process.*, vol. 61, no. 9, pp. 168–182, May 2013.

[35] F. Gustafsson and F. Gunnarsson, "Mobile positioning using wireless networks: Possibilities and fundamental limitations based on available wireless network measurements," *IEEE Signal Process. Mag.*, vol. 22, no. 4, pp. 41–53, Jul. 2005.

[36] U. Hammes, E. Wolsztynski, and A. M. Zoubir, "Robust tracking and geolocation for wireless networks in NLOS environments," *IEEE J. Sel. Topics Signal Process.*, vol. 3, no. 5, pp. 889–901, Oct. 2009.

[37] S. Bartoletti, W. Dai, A. Conti, and M. Z. Win, "A mathematical model for wideband ranging," *IEEE J. Sel. Topics Signal Process.*, vol. 9, no. 2, pp. 216–228, Mar. 2015.

[38] F. R. Hampel, E. M. Ronchetti, P. J. Rousseeuw, and W. A. Stahel, *Robust Statistics: The Approach Based on Influence Functions*. Hoboken, NJ, USA: Wiley, 2005.

[39] S. Tomic and M. Beko, "A bisection-based approach for exact target localization in NLOS environments," *Signal Process.*, vol. 143, pp. 328–335, Feb. 2018.

[40] B. Chen, X. Liu, H. Zhao, and J. C. Principe, "Maximum correntropy Kalman filter," *Automatica*, vol. 76, pp. 70–77, Feb. 2017.